LETTERS

A sharp lithosphere–asthenosphere boundary imaged beneath eastern North America

Catherine A. Rychert[1], Karen M. Fischer[1] & Stéphane Rondenay[2]

Plate tectonic theory hinges on the concept of a relatively rigid lithosphere moving over a weaker asthenosphere, yet the nature of the lithosphere–asthenosphere boundary remains poorly understood. The gradient in seismic velocity that occurs at this boundary is central to constraining the physical and chemical properties that create differences in mechanical strength between the two layers. For example, if the lithosphere is simply a thermal boundary layer that is more rigid owing to colder temperatures, mantle flow models[1,2] indicate that the velocity gradient at its base would occur over tens of kilometres. In contrast, if the asthenosphere is weak owing to volatile enrichment[3–6] or the presence of partial melt[7], the lithosphere–asthenosphere boundary could occur over a much smaller depth range. Here we use converted seismic phases in eastern North America to image a very sharp seismic velocity gradient at the base of the lithosphere—a 3–11 per cent drop in shear-wave velocity over a depth range of 11 km or less at 90–110 km depth. Such a strong, sharp boundary cannot be reconciled with a purely thermal gradient, but could be explained by an asthenosphere that contains a few per cent partial melt[7] or that is enriched in volatiles relative to the lithosphere[3–6].

Precise determination of the thickness of the continental lithosphere and the magnitude and depth range of the velocity gradient at its base has proved challenging with existing seismic techniques. Discontinuities in the 80–210 km depth range have been observed on a regional scale in continental settings by reflection and refraction experiments and by teleseismic body-wave phases[4,8–16], and in some cases these features have been interpreted as the lithosphere–asthenosphere boundary[11–15]. Yet, perhaps because of significant variations in the depth of the discontinuity, an omnipresent discontinuity has yet to be illuminated in global or continental stacks of seismic phases[17]. More significantly, even where the base of the continental lithosphere has been identified[11–15], constraints on the velocity gradient at this boundary have been too loose to permit a clear assessment of its physical and chemical properties.

In this study, we imaged the base of the lithosphere in eastern North America using P-to-S (Ps) conversions produced by scattering of teleseismic P waves at this discontinuity. Ps arrival times may be used to determine discontinuity depths. For example, Ps and S-to-P (Sp) conversions recorded on and near the Hawaiian Islands have successfully identified the base of the lithosphere at depths of 50 km to 110 km (refs 18–20). Furthermore, Ps amplitudes as a function of wave period directly reflect the gradient of velocity with depth, allowing us to probe the mechanisms responsible for the lithosphere–asthenosphere boundary.

Our study region spans the Palaeozoic Appalachian orogen and the eastern coastal margin of the United States (Fig. 1). Following the collision of the proto-African and proto-North American plates, the last major tectonic events to affect the lithosphere in this area were Triassic and Jurassic rifting in the east related to the opening of the Atlantic Ocean[21], and passage of the lithosphere over a plume ~100–120 Myr ago[22]. Surface waves image a seismically fast lithospheric lid in eastern North America that extends to roughly 200 km depth beneath the craton just to the west of our study region, and thins to 80–90 km depth at the continental margin in the east[23,24].

We analysed SV components of Ps conversions recorded by six permanent broadband stations that have been operating for over 5 years (Fig. 1). For each station, the recorded waveforms were decomposed into P and S components using a free-surface transformation matrix and then simultaneously deconvolved in the

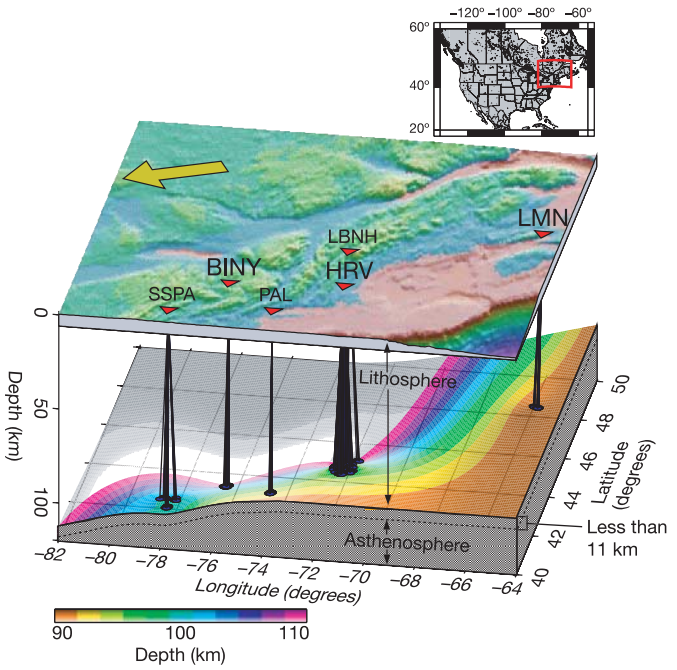

Figure 1 | Three-dimensional view of the lithosphere–asthenosphere boundary and surface topography. Red box in the inset map highlights the location of the study region within North America. Shading on the top surface indicates topography. Yellow arrow points in the direction of absolute plate motion; plate velocity is 2.5 cm yr^{-1}. Red triangles denote station locations. The lower surface represents the location of the base of the lithosphere interpolated from migrated Ps waveform images at the six labelled stations. The larger text corresponds to the stations (HRV, LMN, BINY) where this phase is most clearly observed. This surface ranges from 90 km (orange) to 110 km (pink) depth. Each colour band covers 2 km in depth. Blue circles on the discontinuity surface indicate the conversion points of the Ps phases. Black lines connect piercing points to the station at which the conversion is observed.

[1]Department of Geological Sciences, Brown University, Box 1846, Providence, Rhode Island 02912, USA. [2]Department of Earth, Atmospheric, and Planetary Sciences, Massachusetts Institute of Technology, 77 Massachusetts Avenue, Cambridge, Massachusetts 02139, USA.

frequency domain and migrated to depth, thus illuminating the shear component of energy scattered from velocity discontinuities[8].

A negative phase from depths comparable to the base of the lithosphere is clearly observed at stations HRV, LMN and BINY, and is also apparent at stations PAL, SSPA and LBNH (Fig. 2; Supplementary Information, section 1.1). Synthetic seismograms calculated for the crustal models that best fit the Moho and the first Moho reverberations confirm that crustal phases and their interference cannot mimic the apparent arrival from the base of the lithosphere (Supplementary Information, section 1.1). In addition, the arrival time of the phase at different stations does not consistently correlate with variations in crustal thickness, as would be the case if this phase were related to Moho reverberations. For example, the Moho at station LMN is ~10 km deeper than the Moho at HRV, yet the phase from the base of the lithosphere at LMN migrates to a depth ~7 km shallower than the phase at HRV (Fig. 2). Although variations in the character of the phase occur between stations, they correspond in general to the character of the entire impulse response, and much of this variation is unrelated to the velocity gradient at the discontinuity (Supplementary Information, section 1.1).

The depth of the observed discontinuity ranges from 90 km (LMN) to 110 km (LBNH), increasing to the northwest beneath the Appalachian orogen (Fig. 1) with a landward rather than a seaward[25] dip. Uncertainties on the absolute depth of the discontinuity at each station are less than 1.6 km (Supplementary Information, section 1.1). We associate this phase with the base of the lithosphere, because its depth lies within the transition from fast seismic lid to slow low-velocity zone seen in surface wave tomography[23,24] (Fig. 2).

The Ps phase scattered from the base of the lithosphere requires a very sharp transition between the lithosphere and the asthenosphere. The velocity gradient at the lithosphere–asthenosphere boundary was determined by inverting the migrated waveforms at stations HRV and LMN using a damped least-squares method, assuming a linear gradient (Supplementary Information, section 2). Shallower discontinuities were also modelled to avoid biasing estimates of the lithosphere–asthenosphere gradient, and trade-offs between the absolute depth, depth extent, and magnitude of the lithosphere–asthenosphere gradient were carefully assessed (Supplementary Information, section 2 and Supplementary Table 1). The data at HRV resolve a 3.1–5.7% drop in shear-wave velocity over 5 km or less centred at ~97.0 km depth. The best-fitting models for LMN indicate that the gradient occurs over 5 km or less and the velocity contrast ranges from 6.8% to 7.4% centred at ~90.7 km (Supplementary Table 2). However, thicknesses of almost 11 km cannot be ruled out by 95% confidence limits at LMN, and a thickness of 10 km implies a velocity contrast of 10.7%. Although the depth ranges over which these strong velocity contrasts occur are surprisingly sharp (<11 km), they are well-resolved owing to the relatively short-period energy that dominates the scattered waves (Supplementary Information, section 2).

At station HRV, in addition to the phase from the base of the lithosphere, we observe a phase that is consistent with a negative velocity contrast of 5.4 ± 0.6% at 60.9 ± 0.4 km depth (Supplementary Information, section 2), whereas no discontinuity internal to the mantle lithosphere is observed at LMN. If the observed phase does in fact originate from a discontinuity at 61 km depth below HRV, it may be explained by greater hydration or chemical depletion in the lower lithosphere at HRV than at LMN. However, because the existence of a

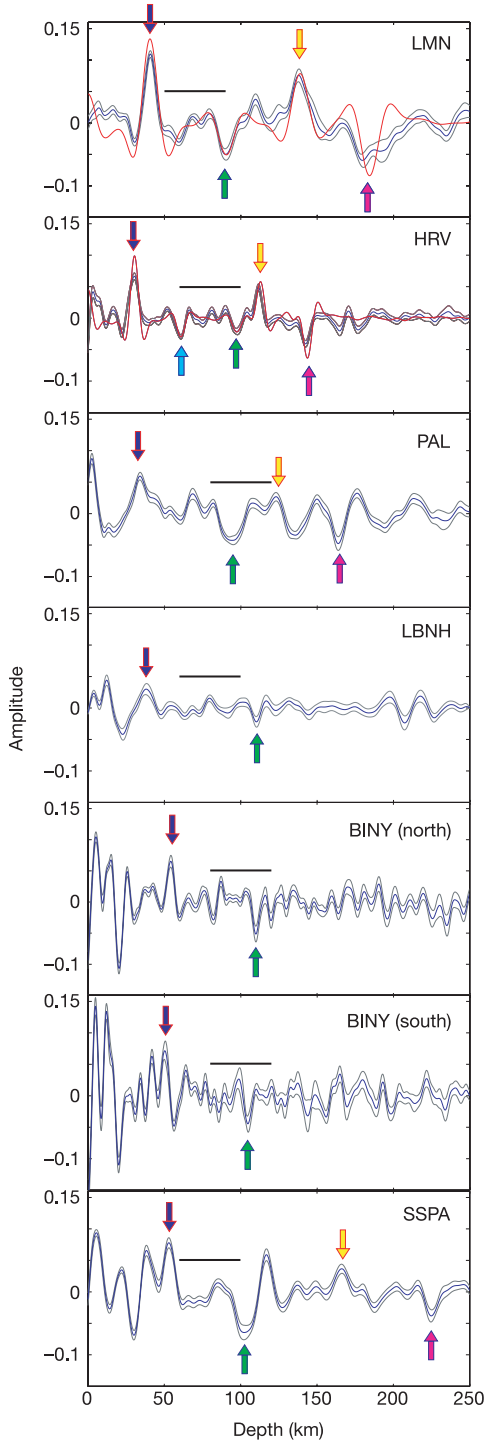

Figure 2 | Imaging discontinuities with waveforms from individual stations. Blue lines show SV waveforms deconvolved and migrated in single bins for stations LMN, HRV, PAL, LBNH, BINY in two back-azimuth bins, and SSPA. A positive phase corresponds to a velocity increase with depth, while a negative phase indicates a velocity decrease with depth. Coloured arrows indicate phases from the base of the lithosphere (green), the Moho (dark blue), crustal reverberations (yellow and magenta), and, for station HRV, a discontinuity at 61 km depth (light blue). Error bars corresponding to two standard deviations (grey lines) were calculated with bootstrap tests in which a random 20% of the events in the bin were randomly replaced by another 20%, and the deconvolved, migrated waveforms were recalculated 100 times. Horizontal black lines correspond to the lithosphere–asthenosphere boundary as determined by surface wave models, defined as the greatest negative velocity gradient (LMN[23], all others[24]). Synthetic waveforms corresponding to the models obtained by inverting the data are shown for HRV and LMN (red lines). Crustal phase amplitudes were not included in these inversions and are therefore the one aspect of the synthetic waveforms that do not match the data (Supplementary Information, section 2).

61 km discontinuity is ambiguous (Supplementary Information, section 1.2), we modelled the velocity drop at the lithosphere–asthenosphere boundary beneath HRV with and without a 61 km discontinuity, and found that a similar velocity contrast is required (3.3–5.7% and 3.1–4.9%, respectively; Supplementary Table 2).

At the lithosphere–asthenosphere boundary, the shear-wave velocity contrasts that best fit the Ps scattering (3.1–7.4%) are comparable to surface wave studies in which the total drop in velocity from the lithospheric lid to the slower asthenosphere varies from 3% to 11% across the region[23,24]. However, these same surface wave studies cannot clearly resolve the difference between sharp velocity gradients and those that occur over ~40–50 km. Our results require that the velocity contrast occurs over less than 11 km. In addition, the shear-wave velocity drop at the base of the lithosphere in this continental orogen/margin environment is similar to that found in old Pacific oceanic lithosphere using joint surface-wave and body-wave inversions (6.4%); yet, again the Ps scattering requires a sharper gradient ($<$11 km versus $<$30 km; ref. 4). Reflection studies in localized zones at the base of the continental or passive margin lithosphere have invoked gradients over comparable depth ranges[15], but they did not model the magnitude of the velocity drop. Another Ps study[26] that included station HRV did not notice a phase from the base of the lithosphere because the elimination of higher frequencies in the study caused crustal reverberations to destructively interfere with the phase from the base of the lithosphere (Supplementary Information, section 1.1).

What mechanisms could be responsible for the strong, sharp velocity gradient associated with the base of the lithosphere? Experimental studies[27] suggest that if the velocity gradient is caused solely by temperature, temperature increases of at least 220 °C and 120 °C are required to explain the velocity contrasts at LMN and HRV, respectively (Supplementary Information, section 3). However, numerical models of mantle flow in which viscosity depends only on temperature and pressure indicate that the thermal gradient at the base of the lithosphere is typically less than 5 °C km^{-1}, and definitely less than 10 °C km^{-1} (refs 1, 2). These models are not able to match the greater than 20 °C km^{-1} temperature gradient that would be required at the base of the lithosphere at LMN and HRV, and another mechanism besides temperature is required to explain the observed velocity contrast.

A vertical variation in mantle chemical composition—for example, a lithosphere dehydrated and depleted in Fe, Ca and Al owing to past melt extraction versus an undepleted, volatile-rich asthenosphere[3–6]—could produce a sharp enough discontinuity. Here we assume that mantle temperatures are sub-solidus. The maximum possible shear-wave velocity variation due to depletion is ~1.5% (ref. 28). Because hydration reduces velocity primarily by increasing attenuation[5], its effect is limited by reasonable attenuation contrasts between the lithosphere and asthenosphere and is no more than roughly 4.3% (Supplementary Information, section 3). Depletion and hydration are therefore individually too small to explain the 6.8–7.4% velocity drop inferred from the best-fitting models at LMN. However, a velocity contrast caused by the combination of dehydration and depletion encompasses the HRV values (3.3–5.7%) and could reach the LMN range with a modest contribution from temperature. A sharp decrease in grain size with depth could also reduce velocity[27], but because grain size, like hydration, affects velocity via attenuation, the total contribution from hydration and grain size still cannot exceed ~4.3%.

Another possibility is that the strong, sharp lithosphere–asthenosphere boundary is produced by the presence of small amounts of partial melt in the asthenosphere, which could easily produce the roughly 7% velocity drop inferred for the best-fitting LMN models and even the 11% velocity drop associated with the largest gradient thickness permitted by the LMN data[29] (Supplementary Information, section 3). In this scenario, the lithosphere–asthenosphere boundary is defined by the solidus, preventing melt from rising into the lithosphere. One mechanism for generating melt beneath eastern North America is decompression of mildly hydrated[3] (an atomic ratio of 800–1,000 H per 10^6 Si) asthenospheric material as it flows upward along the contours of the more rigid, shallowing lithosphere in response to the west-southwest absolute motion of the North American plate[30] (Fig. 1). Melt would be continually regenerated by rising hydrated asthenosphere, replacing any melt carried out of the region by solid mantle flow or lost via melt migration and cooling. Alternatively, temperatures may exceed the damp-solidus within the asthenosphere without the need for decompression. In these scenarios involving asthenospheric melting, or those in the preceding paragraph at sub-solidus conditions, temperature will also contribute to the observed velocity gradient, and because melt and/or compositional boundaries would produce rapid decreases in viscosity with depth[3], temperature gradients could be sharper than in models where viscosity depends solely on temperature and pressure[1,2].

In the future, comparing well-resolved velocity gradients at the base of the lithosphere between a variety of tectonic environments should help to isolate the relative roles of temperature, hydration, depletion and melting. On the basis of the present study, however, we are able to conclude that the strong, sharp lithosphere–asthenosphere boundary beneath this continental region cannot be defined solely by temperature, but is consistent with a rapid rheological transition produced by melt or volatiles in the asthenosphere.

Received 23 November 2004; accepted 20 May 2005.

1. King, S. D. & Ritsema, J. African hot spot volcanism: small scale convection in the upper mantle beneath cratons. *Science* **290,** 1137–1140 (2000).
2. Zaranek, S. E., Parmentier, E. M. & Fischer, K. M. Effects of basal drag and ablation on the evolution of cratonic lithosphere. *Eos* **85**(17), T41C–03 (2004).
3. Hirth, G. & Kohlstedt, D. L. Water in the oceanic upper mantle; implications for rheology, melt extraction and the evolution of the lithosphere. *Earth Planet. Sci. Lett.* **144,** 93–108 (1996).
4. Gaherty, J. B., Kato, M. & Jordan, T. H. Seismological structure of the upper mantle; a regional comparison of seismic layering. *Phys. Earth Planet. Inter.* **110,** 21–41 (1999).
5. Karato, S.-I. & Jung, H. Water, partial melting and the origin of the seismic low velocity and high attenuation zone in the upper mantle. *Earth Planet. Sci. Lett.* **157,** 193–207 (1998).
6. Hirth, G., Evans, R. L. & Chave, A. D. Comparison of continental and oceanic mantle electrical conductivity: Is the Archean lithosphere dry? *Geochem. Geophys. Geosyst.* **1,** 2000GC00048 (2000).
7. Anderson, D. L. *Theory of the Earth*, (Blackwell Scientific, Boston, Massachusetts, 1989).
8. Bostock, M. G. Mantle stratigraphy and evolution of the Slave province. *J. Geophys. Res.* **103,** 21183–21200 (1998).
9. Dueker, K., Yuan, H. & Zurek, B. Thick-structured Proterozoic lithosphere of the Rocky Mountain region. *GSA Today* **11,** 4–9 (2001).
10. Revenaugh, J. & Jordan, T. H. Mantle layering from ScS reverberations; 3, The upper mantle. *J. Geophys. Res.* **96,** 19781–19810 (1991).
11. MONA LISA Working Group, MONA LISA—Deep seismic investigations of the lithosphere in the southeastern North Sea. *Tectonophysics* **269,** 1–19 (1997).
12. Morozova, E. A., Morozov, I. B., Smithson, S. B. & Solodilov, L. N. Heterogeneity of the uppermost mantle beneath Russian Eurasia from the ultra-long-range profile QUARTZ. *J. Geophys. Res.* **104,** 20329–20348 (1999).
13. Ryberg, T. *et al.* Two-dimensional velocity structure beneath northern Eurasia derived from the super long-range seismic profile Quartz. *Bull. Seismol. Soc. Am.* **86,** 857–867 (1996).
14. Steer, D. N., Knapp, J. H. & Brown, D. L. Super-deep reflection profiling: exploring the continental mantle lid. *Tectonophysics* **286,** 111–121 (1998).
15. Steer, D. N. *et al.* Deep structure of the continental lithosphere in an unextended orogen; an explosive-source seismic reflection profile in the Urals (Urals Seismic Experiment and Integrated Studies (URSEIS 1995)). *Tectonics* **17,** 143–157 (1998).
16. Thybo, H. & Perchuc, E. The seismic 8° discontinuity and partial melting in continental mantle. *Science* **275,** 1626–1629 (1997).
17. Shearer, P. M. Constraints on upper mantle discontinuities from observations of long-period reflected and converted phases. *J. Geophys. Res.* **96,** 18147–18182 (1991).
18. Li, X. *et al.* Mapping the Hawaiian plume conduit with converted seismic waves. *Nature* **405,** 938–941 (2000).
19. Collins, J. A. *et al.* Broadband seismology in the oceans; lessons from the ocean seismic network pilot experiment. *Geophys. Res. Lett.* **28,** 49–52 (2001).
20. Li, X., Kind, R., Yuan, X., Wolbern, I. & Hanka, W. Rejuvenation of the lithosphere by the Hawaiian plume. *Nature* **427,** 827–829 (2004).

21. Hatcher, R. D. Jr in *The Appalachian-Ouachita Orogen in the United States* (eds Hatcher, R. D. Jr, Thomas, W. A. & Viele, G. W.) 511–519 (Geological Society of America, Boulder, Colorado, 1989).
22. Heaman, L. M. & Kjarsgaard, B. A. Timing of eastern North American kimberlite magmatism; continental extension of the Great Meteor Hotspot track? *Earth Planet. Sci. Lett.* **178,** 253–268 (2000).
23. Van der Lee, S. High-resolution estimates of lithospheric thickness from Missouri to Massachusetts, USA. *Earth Planet. Sci. Lett.* **203,** 15–23 (2002).
24. Li, A., Forsyth, D. W. & Fischer, K. M. Shear velocity structure and azimuthal anisotropy beneath eastern North America from Rayleigh wave inversion. *J. Geophys. Res.* **108,** doi:10.1029/2002JB02259 (2003).
25. Menke, W. & Levin, V. Anomalous seaward dip of the lithosphere-asthenosphere boundary beneath northeastern USA detected using differential-array measurements of Rayleigh waves. *Geophys. J. Int.* **149,** 413–421 (2002).
26. Li, A., Fischer, K. M., van der Lee, S. & Wysession, M. E. Crust and upper mantle discontinuity structure in eastern North America. *J. Geophys. Res.* **107,** doi:10.1029/2001JB000190 (2002).
27. Jackson, I., Fitz Gerald, J. D., Faul, U. H. & Tan, B. H. Grain size sensitive sesmic wave attenuation in polycrystalline olivine. *J. Geophys. Res.* **107,** doi:10.1029/2001JB001225 (2002).
28. Lee, C.-T. A. Compositional variation of density and seismic velocities in natural peridotites at STP conditions: Implications for seismic imaging of compositional heterogeneities in the upper mantle. *J. Geophys. Res.* **108,** doi:10.1029/2003JB002413 (2003).
29. Hammond, W. C. & Humphreys, E. D. Upper mantle seismic wave velocity; effects of realistic partial melt geometries. *J. Geophys. Res.* **105,** 10975–10986 (2000).
30. Fouch, M. J., Fischer, K. M., Parmentier, E. M., Wysession, M. E. & Clarke, T. J. Shear wave splitting, continental keels, and patterns of mantle flow. *J. Geophys. Res.* **105,** 6255–6275 (2000).

Supplementary Information is linked to the online version of the paper at www.nature.com/nature.

Acknowledgements We thank L. Elkins-Tanton, D. W. Forsyth and G. Hirth for discussions. Data came from the IRIS Global Seismic Network, the US National Seismic Network, the Canadian National Seismic Network, and the Lamont Seismic Network. The National Science Foundation Geophysics Program provided support for this project.

Author Information Reprints and permissions information is available at npg.nature.com/reprintsandpermissions. The authors declare no competing financial interests. Correspondence and requests for materials should be addressed to C.R. (Catherine_Rychert@Brown.edu).